# Nonlinear site response and strain-dependent soil properties

**Takaji Kokusho**

Department of Civil Engineering, Faculty of Science and Engineering, Chuo University, Tokyo 112, Japan

**Vertical array records obtained during the 1995 Kobe earthquake were utilized to study seismic site amplification during destructive earthquakes. Spectrum ratios between ground surface and deeper levels were calculated for the main shock and associated small shocks to demonstrate significant effect of soil nonlinear properties on site response. The records are back-calculated to evaluate *in situ* strain-dependent soil properties to be compared with laboratory test data. Shear moduli and damping ratios of soil layers to best reproduce the seismic response are back-calculated by means of an inversion analysis. Clear strain-dependent modulus degradations which can be differentiated for different soil types are recognized. The degradations and damping variations are essentially consistent with laboratory test results for each soil type, although further quantitative study is still needed, particularly for damping.**

LOCAL site amplification is one of the most important factors in seismic zonation studies. The site amplification is correlated not only to soil thicknesses but also to soil properties such as shear modulus and damping as well as soil densities. At the same time, it is highly dependent on the strain-dependent nonlinearity of soil properties at soft soil sites during destructive earthquakes. This nonlinear effect did not draw so much attention for a long time by seismologists in particular because wave-transmitting media had historically been idealized as elastic in seismology. In the 1970s, analytical tools for seismic response of soft ground due to nonlinear soil properties were already available either by equivalent linear analyses[1] or step-by step nonlinear analyses[2]. Shake table tests for model ground in a laminar shear box either in 1g tests or by centrifuge tests repeatedly demonstrated a clear reduction in dynamic amplification due to nonlinear soil properties by increasing input acceleration level[3]. Laboratory soil tests for dynamic soil properties developed in the past three decades disclosed that soils change from a linear material to a nonlinear material as induced shear strain grows from $10^{-6}$ to $10^{-3}$ and finally reach failures at strain larger than $10^{-2}$; Shear modulus $G$ and damping ratio $D$ change as schematically shown in Figure 1 *a*. In current engineering practice, shear modulus $G$ is normalized by initial shear modulus $G_0$ ($G_0 = \rho V_s^2$: where $V_s$ = elastic S-wave velocity and $\rho$ = soil density) and the modulus degradation curve is drawn as shown in Figure 1 *b*. This considerable properties change no doubt gives a great effect on seismic site response. However, due to absence of actual strong motion records, the degree of nonlinearity actually associated with destructive earthquakes has long been subject to discussions among researchers from different disciplines including earthquake engineering and seismology. During the 1995 Hyogoken Nambu earthquake (sometimes called as the Kobe earthquake), a set of valuable vertical array records were obtained, which could demonstrate significant effect of soil nonlinearity on site response. The records also served to back-calculate strain-dependent changes of *in situ* soil properties. In this article, I summarize recent research findings on nonlinear site response and *in situ* soil properties.

## Vertical arrays and spectrum ratios

Vertical arrays, which could record the 1995 Hyogoken-Nambu (Kobe) earthquake ($M_J$ = 7.2: the Japanese Earthquake Magnitude almost equivalent to the Richter's Magnitude) were located at four sites; PI, SGK, TKS and KNK in the coastal zone around the Osaka Bay area as shown

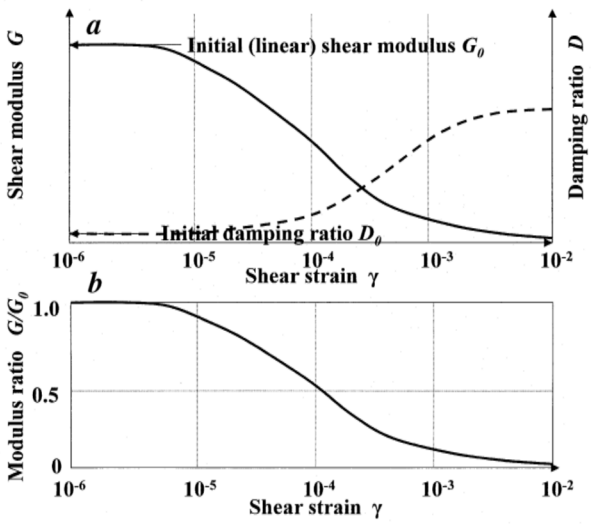


**Figure 1.** Shear modulus/damping ratio versus shear strain relationship (***a***) and modulus degradation curve (***b***).

e-mail: kokusho@civil.chuo-u.ac.jp

in Figure 2. The same figure also indicates the fault zone including the epicenters of the main-shock as well as aftershocks. The four sites were located in different distances from the causative fault. In Figure 3, maximum acceleration distributions for the main shock along the depth of vertical arrays at the four sites are illustrated in the two horizontal directions and one vertical direction. The accelerations are extremely different from site to site due to different focal distances, leading to different amplifications[4]. In the farthest site, KNK, where the horizontal surface ground acceleration is around 0.1 g, the amplitude increases quite normally with decreasing depth, while in the nearest site, PI, where the horizontal acceleration is around 0.5 g at the depth of 84 m, the acceleration does not show clear increase with decreasing depth and drastically decreases at the surface due to extensive liquefaction occurring in a man-made surface layer. In other sites, the amplifications are characterized as in between PI and KNK.

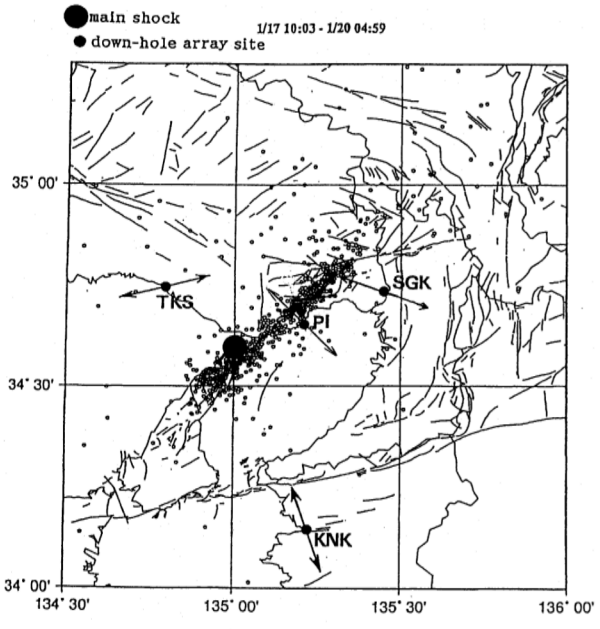


**Figure 2.** Location of vertical array sites around Osaka Bay and epicenters of main-shock and aftershocks (Arrows indicate principal axes of maximum horizontal accelerations).

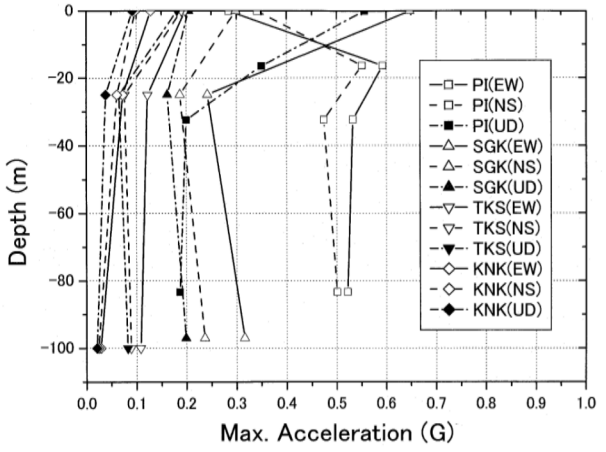


**Figure 3.** Maximum accelerations along depth in two horizontal and one vertical directions at 4 vertical array sites.

The soil profiles and the installation depths of down-hole seismographs are shown for individual sites in Figure 4 *a–d* together with the P and S-wave velocities measured by the down-hole logging method and the SPT N-values along the depth. The deepest seismographs at the base layers were located GL-97m at SGK, GL-83m at PI, and GL-100m at TKS and KNK respectively, and the geological conditions at the depths were Pleistocene dense gravelly soils except for KNK where the base layer consists of hard rock. Upper soil conditions at the four sites mostly consist of sandy fill at the surface underlain by Holocene clay and/or sand and further underlain by Pleistocene soils. The S-wave velocity, $V_s$, at the base layer of Pleistocene gravelly soil at PI, SGK and TKS is 380–480 m/s while $V_s$ at the base rock at KNK is as high as 1630 m/s.

At each site, several small shock records (including aftershocks and small events before the main shock not necessarily foreshocks) as well as the main shock record were used for evaluating spectrum ratios. Fourier spectra of seismic records obtained at the ground surface and deeper levels of the vertical arrays were calculated by the Fast Fourier Transform scheme and their ratios were computed to have the spectrum ratios between ground surfaces and base layers. In Figure 5 *a–d*, spectrum ratios calculated for the main shock at the four sites are compared with those of the small shocks in terms of their average and the average plus or minus the standard deviation. The spectrum ratios for the main shock are mostly smaller than those for the aftershocks although they are closer or sometimes reverse in the first peak. Peak frequencies of the main shock tend to be lower than those of the small shocks at most sites. This trend is more pronounced in the second or higher frequency peaks than in the first peak presumably because soil nonlinearity is more dominant in shallower layers, which influences higher frequency peaks more than lower ones. The differences in spectrum ratios and peak frequencies between the main shock and the small shocks tend to be narrowed as the vertical array sites are getting remote from the causative fault; from the nearest PI, to the farthest KNK.

## Laboratory soil tests

Numerous laboratory tests have been conducted to date since the pioneering work by Seed and Idriss[5] to establish the strain-dependent changes of modulus and damping on different types of soils. For example, Iwasaki and Tatsuoka[6] conducted cyclic loading torsional shear tests of reconstituted

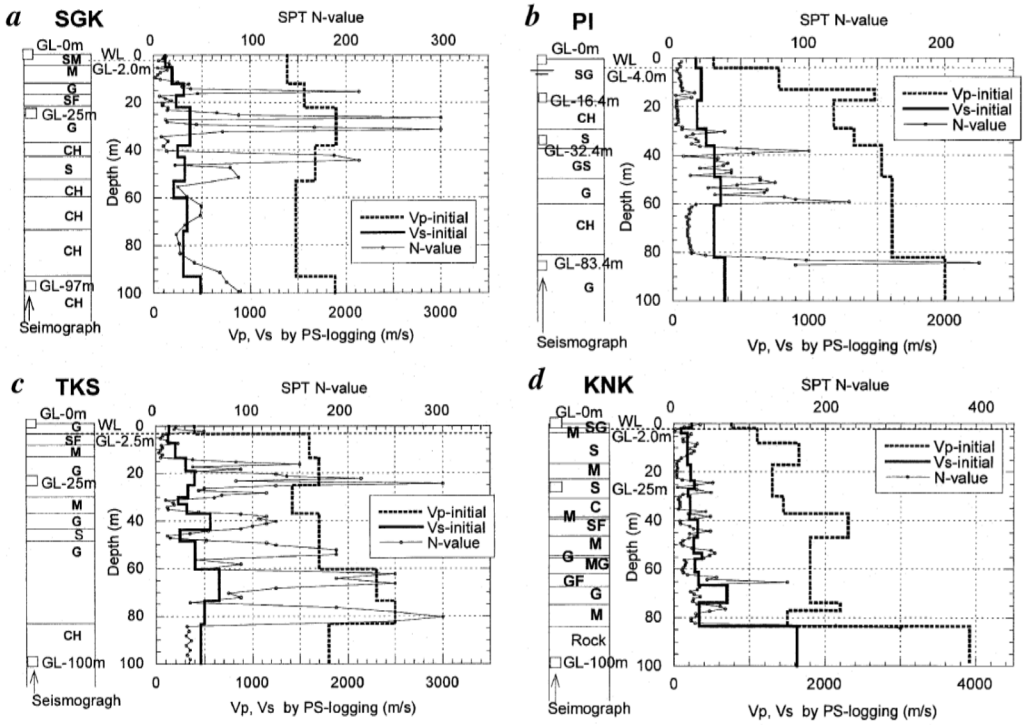


**Figure 4.** Soil profiles and installation depths of down-hole seismographs with P and S-wave velocities and SPT N-values.

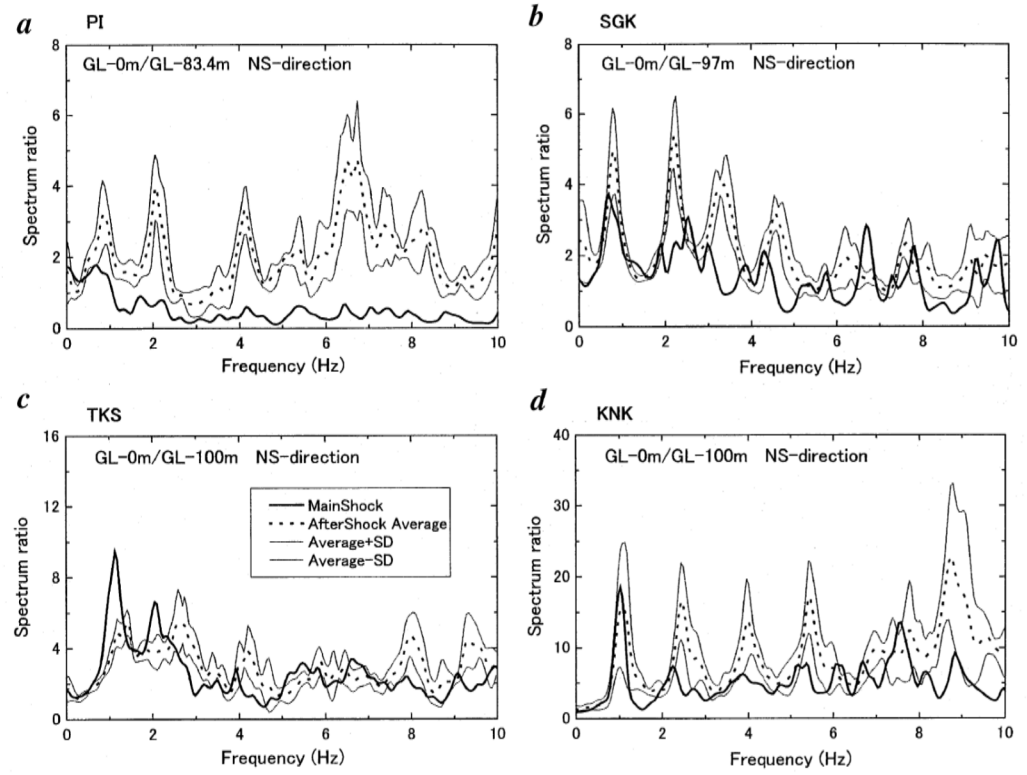


**Figure 5.** Spectrum ratios (between surface and base layer) for the main shock compared with small shocks at 4 sites.

sand specimens in which shear moduli and hysteretic damping ratios were measured in a wide strain range from $10^{-6}$ to $10^{-2}$. Improved cyclic triaxial tests were carried out[7–10] for sands, clays and gravels in which inner load cells and high sensitivity proximity sensors were introduced inside pressure chambers, as illustrated in Figure 6, so that soil properties could be measured for a wide strain range from $10^{-6}$ to $10^{-2}$ without unfavourable effect of mechanical frictions. Based on a series of such tests, empirical curves correlating shear modulus ratio $G/G_0$ with log $\gamma_{eff}$ for clays, sands and gravels are shown in Figure 7 *a–c*, respectively. In the light of accumulated data of quite a few similar laboratory tests, it is generally accepted at present that the modulus degradation curves for sands are positioned more left than those for clays and those of gravels are positioned further left than sands on the $G/G_0$ versus log $\gamma_{eff}$ chart. For clay, plasticity index, $I_p$, is known as a decisive factor of modulus degradation curves of clays (e.g. ref. 8); larger $I_p$ gives milder degradation rate at the same effective strain. Furthermore, the curves for sands and gravels tend to shift rightward with increasing confining pressures. In the following, the back-calculated strain-dependent variations are compared with laboratory values.

## Strain-dependency of back-calculated *in situ* properties at 4 sites

Strain-dependent soil properties were back-calculated by a computer code developed by Suetomi[11] based on the Extended Bayesian method. Not only the main shock records but also small shock records are analysed to have better estimation of variations of *in situ* soil properties with varying seismic intensity. Further details on the back-calculation are available in other literatures[12,13].

In Figure 8 *a* and *b*, data points of the back-calculated modulus ratios and damping ratios for different types of soils are plotted versus effective strain $\gamma_{eff}$, respectively. The plots represent properties of individual soil layers in the soil profiles at the four sites illustrated. The soil classifications here are based on the Unified Soil Classification System, and C (CH), M, S (SF, SG) and G(GF, GS) stand for clay, silt, sand and gravel, respectively. Clear strain-dependent modulus degradations can be recognized for every soil type despite some data dispersions. The data points encircled in Figure 8 *a* correspond to sandy decomposed granite in PI which extensively liquefied during the main shock and hence experienced considerable modulus decrease and strain increase. For sands and gravels, the values of $\gamma_{eff}$ in the horizontal axis are normalized as $\gamma_{eff}/(\sigma_c'/p_0)^{0.5}$ in order to cancel the effect of confining stress. Figure 8 *a* clearly indicates that clays are obviously positioned far right, whereas gravels are located far left despite large scatters in the data points. Silts and sands can be judged to stand between the two soils despite large dispersions. Thus, the clear difference in modulus degradation depending on soil types in the laboratory can also be recognizable in the back-calculated soil properties.

Figure 8 *b* shows that damping ratios stay almost constant up to the strain of about $10^{-4}$ and start to increase for strains larger than that. It should be pointed out that damping ratios for small strain are split into two groups (4–6 and 1–2%, respectively). It is not clear if this difference reflects actual site-specific differences in soil properties or some other factors. Also noted is that damping ratios of gravels are larger than sands and those of sands are larger than clays for larger strain levels, presumably reflecting a similar trend in laboratory tests[8].

Strain-dependent variations of shear modulus ratios and damping ratios back-calculated for different soil types are compared with laboratory test data in Figure 8 *a* and *b*, respectively. The back-calculated properties of clays are compared with laboratory curves based on the test results of intact alluvial clays[9]. In comparing them, it should be borne in mind that the majority of $I_p$-values of clays around the studied area take 80 and 40, while those of the laboratory test data are $I_p$ = 40 to 83 and almost coincidental. Agreement of the degradation curves is very good for $G/G_0$ = 0.5 or larger as indicated in Figure 8 *a*. Curves of laboratory tests for sands by Iwasaki *et al.*[6], Kokusho[7] and Seed *et al.*[14] are drawn to compare with the back-cal-

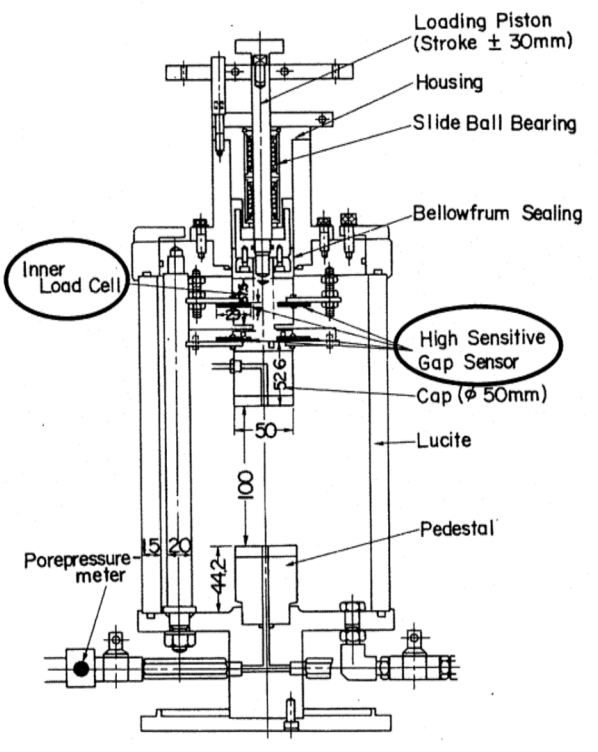


**Figure 6.** Improved cyclic triaxial test apparatus with inner load cells and high sensitivity proximity sensors.

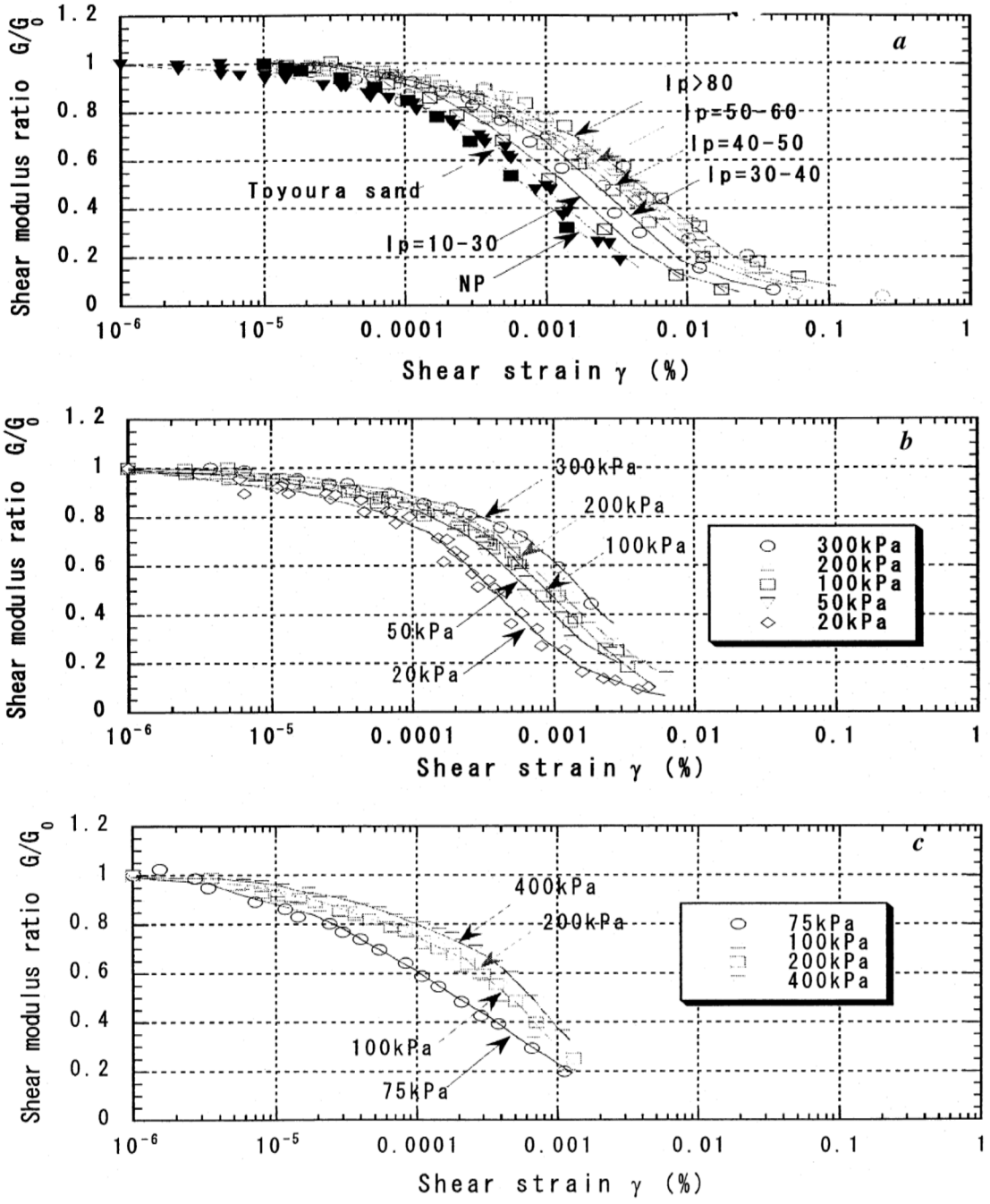


**Figure 7.** Empirical curves correlating shear modulus ratio $G/G_0$ with log $\gamma_{eff}$ for clays (*a*), sands (*b*) and gravels (*c*).

culated results in Figure 8 *a*. The effective confining stress is $\sigma_c' = 98$ kPa. Note that the back-calculated modulus degradation shows a fair agreement with one or two laboratory curves for $G/G_0 \approx 0.5$ or larger. The curve by Seed *et al.*[14] will result in too strong nonlinear effect, though it might be a good estimate for modulus degradation corresponding to extensive liquefaction which took place at the PI-site. Back-calculated properties of silts are in between the two degradation curves for clay and sand, indicating a good consistency between *in situ* and laboratory for silts. For gravels, the back-calculated modulus degradation is obviously milder than the laboratory curves. This may possibly be attributed to the fact that actual gravel soils, unlike pure gravels in the laboratory, normally contain

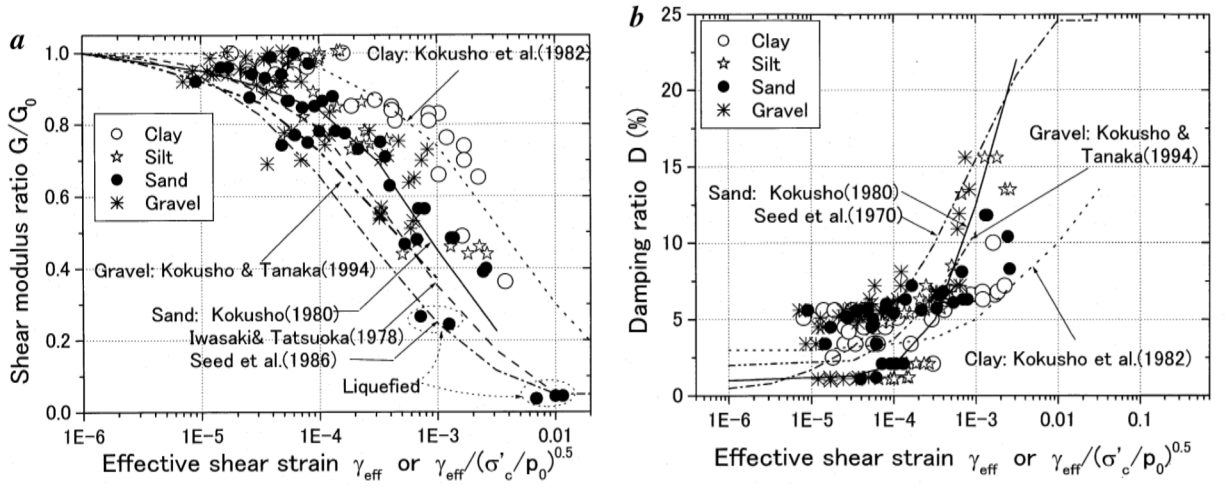


**Figure 8.** Back-calculated modulus ratios (***a***) and damping ratios (***b***) for different soils plotted versus effective strain $\gamma_{eff}$ compared with previous lab test data.

appreciable amount of finer soils and tend to share some of their properties.

With regard to damping ratios in Figure 8 *b*, the agreement between *in situ* and laboratory is evidently poorer than modulus degradations though the back-calculated damping ratios share clear trends of increasing damping with increasing strain. The majority of the back-calculated damping ratios are plotted a few percent higher than most laboratory test results, particularly in a strain range smaller than $10^{-4}$. For clays, *in situ* damping values tend to increase with increasing strain almost in parallel with the laboratory curve up to $\gamma_{eff} = 3 \times 10^{-3}$ but the former is larger than the latter by about two percent. In other soil types, the clear split in the back-calculated damping values in the small strain range makes straightforward comparison difficult, indicating further research needs for more reliable *in situ* damping evaluation. Note that the damping ratio is assumed as frequency-independent as a normal geotechnical engineering practice. The effect of frequency-dependency of damping, which cannot be ignored in observed seismic records, should also be investigated further.

## Conclusions

It has been demonstrated from maximum acceleration distribution along depth and also from spectrum ratios that seismic site amplification strongly reflects nonlinear soil properties during destructive earthquakes. In particular, liquefaction de-amplifies surface accelerations. Clear modulus degradations can be identified *in situ* by back-calculation, which are almost consistent at the four sites and can be differentiated for clay, silt, sand and gravel, respectively. Back-calculated damping ratios clearly increase with increasing strain range larger than $10^{-4}$ but stay almost constant in the smaller strains although the values are widely diverged from 1% to 6%. A good agreement in modulus degradation can be recognized between back-calculation and some of previous laboratory test results for clays and sands unless the degradation exceeds around $G/G_0 = 0.5$. For gravels, milder back-calculated degradations are obtained than laboratory tests, presumably reflecting appreciable fine soils content. The majority of the back-calculated damping ratios are a few per cent higher than laboratory test results particularly in small strain ranges. Apparent splits in the back-calculated damping values in small strain ranges indicates further research needs for more reliable *in situ* damping evaluation.


1. Schnabel, P. B., Lysmer, J. and Seed, H. B., SHAKE, A computer program for earthquake response analysis of horizontally layered sites. Report EERC 72-12, University of California Berkeley, 1972.
2. Constantopoulos, I. V., Roesset, J. M. and Christian, J. T., A comparison of linear and exact nonlinear analyses of soil amplification. Proceedings of the 5th International Conference of SMFE, Rome, 1973, pp. 1806–1815.
3. Kokusho, T. and Iwatate, K., Scaled model tests and numerical analyses on nonlinear dynamic response of soft grounds. *J. Jpn Soc. Civil Eng.* (in Japanese), 1979, **III/285**, 57–67.
4. Kokusho, T. and Matsumoto, M., Nonlinearity in site amplification and soil properties during the 1995 Hyogoken-Nambu earthquake. *Soil Found.*, 1998, 1–10.
5. Seed, H. B. and Idriss, I. M., Soil moduli and damping factors for dynamic response analysis, Report EERC 70-10, University of California Berkeley, 1970.
6. Iwasaki and Tatsuoka, F., Shear moduli of sands under cyclic torsional shear loading. *Soil Found.*, 1978, **18**, 39–56.
7. Kokusho, T., Cyclic triaxial test of dynamic soil properties for wide strain range. *Soil Found.*, 1980, **20**, 45–60.
8. Kokusho, T., Dynamic soil properties and nonlinear seismic response of ground, Ph D dissertation, Tokyo University, 1982.
9. Kokusho, T., Yoshida, Y. and Esashi, Y., Dynamic soil properties of soft clay for wide strain range. *Soil Found.*, 1982, **22**, 1–18.

10. Kokusho, T. and Tanaka, Y., Dynamic properties of gravel layers investigated by *in-situ* freezing sampling. Geotechnical Special Publication No 44 – Ground Failures under Seismic Conditions, ASCE Convention (Atlanta), 1994, pp. 121–140.
11. Suetomi, I., A program manual for optimization of soil structure by Bayes Method. Central Research Institute of Sato Kogyo Com. Ltd, 1997.
12. Aoyagi, T., Inversion analysis for soil properties based on vertical array record using the extended Bayesian method, Master's thesis, Graduate School of Chuo University, 2000.
13. Kokusho, T. and Aoyagi, T., *In situ* nonlinear soil properties back-calculated from vertical array records of 1995 Kobe earthquake, Proceedings of the International Conference on *in situ* Measurement of Soil Properties and Case Histories, Indonesian Geotechnical Society, Bali, 2001, pp. 473–480.
14. Seed, H. B., Wong, R. T., Idriss, I. M. and Tokimatsu, K., Moduli and damping factors for dynamic analyses of cohesionless soils. *J. Geotech. Eng.*, 1986, **112**, 1016–1032.
15. Elgamal, A., Lai, T., Yang, Z. and He, L., Dynamic soil properties, seismic downhole arrays and applications in practice. Proceedings of the 4th International Conference on Recent Advances in Geotechnical Earthquake Engineering and Soil Dynamics, San Diego, 2001.
16. Kokusho, T., Sato, K. and Matsumoto, M., Nonlinear dynamic soil properties back-calculated from strong motions during Hyogoken-Nambu Earthquake. Proceedings of the 11th World Conference on Earthquake Engineering, Acapulco, CD publication, 1996.

ACKNOWLEDGEMENTS. Dr Suetomi, I. of National Research Institute for Earthquake Science and Disaster Prevention who kindly provided the computer program of the Extended Bayesian method and helped this analytical research is gratefully acknowledged. The Kansai Electric Power Company and the Kobe Municipal Office who successfully obtained the vertical array records and the Committee of Earthquake Observation and Research in Kansai Area (CEORKA) which generously disseminated them are appreciated with gratitude.